

Joint Reconstruction of Image and Motion for PET Using Linear Diffusion Regularization

M. Blume^{1,2}, M. Rafecas Lopez¹

¹ Instituto de Física Corpuscular (IFIC), CSIC/Universidad de Valencia

² Computer Aided Medical Procedures (CAMP), Technische Universität München

Abstract

We present a modification of our recently proposed joint reconstruction algorithm for PET. A problem related to the original presentation is the need of a regularization parameter which defines the trade-off between data term and regularization term. This regularization parameter is hard to find and usually there is no other way than trying different values and finally choosing the one which leads to the most satisfactory reconstruction. In our modified version, we eliminate the regularization parameter. Both quantitative and visual comparison show that the modified version of our joint reconstruction algorithm provides the same reconstruction quality and is therefore an acceptable substitute.

1 Introduction

We recently presented a novel motion compensation method which jointly reconstructs both image and motion in PET based on dual gated (respiratory and cardiac) data [1].

The term “Joint reconstruction” refers to the fact that image and motion are not separately reconstructed (as this is done in most other methods), but rather in an unseparable joint manner. It is based on a motion-aware likelihood function which depends on both the image and the motion as a parameter. We seek an image and motion which maximize this likelihood function.

Image reconstruction is an ill-posed problem, and image reconstruction including motion even more so. Therefore, we need to apply regularization in order to restrict the solution space to physically reasonable images and motion functions. Physically reasonable motions in our targeted domain are smooth, and so smoothness is one of the constraints enforced by regularization. Furthermore, our algorithm needs the inverse of the motion function during its calculation steps, and so we also require the motion to be invertible at any iteration.

In [1] we added a smoothing term to the likelihood function. The smoothing term is high for smooth motion and low for non-smooth motion functions, and thus encourages smooth motion functions over non-smooth ones. The smoothing term is weighted by a so-called regularization parameter α , which defines the trade-off between the likelihood term and the smoothing term.

A problem related to this approach is that it is not easy to find the correct parameter α . In this paper we investigate a

new approach which does not model the smoothing in the objective function but rather applies Gaussian post-smoothing after each motion update.

2 Methods

2.1 Joint Reconstruction with Perona-Malik Diffusion Regularization (JR-PMD)

In the following, we shortly recall our joint reconstruction approach. We start with a cost functional which depends on both an image and a motion function and is minimal for a good fit of image and motion to the data. As a measure of fit, we use an adapted motion-aware likelihood function. Additionally, a regularization term which encourages spatially smooth motion is used.

Then, we derive an iterative algorithm for minimizing this cost functional. The algorithm basically consists of two update equations (one for the image and one for the motion function) which are repeated.

2.1.1 Cost Functional

In the case of a moving anatomy, an image f can be modeled as $f(\varphi(\mathbf{x}, t))$, where φ is a deformation function $\varphi : \mathbb{R}^4 \mapsto \mathbb{R}^3$ which maps a position \mathbf{x} in space at time t to a new position $\varphi(\mathbf{x}, t)$ in the reference frame. Accordingly, f corresponds to the (virtual) reference/reconstruction frame. The number of measured events $g(a, t)$ of line-of-response a at time frame t are Poisson distributed:

$$P(g(a, t)|f, \varphi) = e^{-\hat{g}(a, t)} \cdot \frac{\hat{g}(a, t)^{g(a, t)}}{g(a, t)!}, \quad (1)$$

where $\hat{g}(a, t) = \frac{1}{T} \int H(a, \mathbf{x}) f(\varphi(\mathbf{x}, t)) d\mathbf{x}$ is the expected number of counts in LOR a at time t given an image f and transformation φ .

The likelihood function for all measured events is

$$L(f, \varphi) = \prod_{a, t} P(g(a, t)|f, \varphi). \quad (2)$$

We seek to find a pair of image f and motion φ that maximizes the likelihood function. This is equivalent to minimizing the negative log-likelihood function

$$-\log(L(f, \varphi)) = \sum_{a,t} \hat{g}(a, t) - g(a, t) \log(\hat{g}(a, t)) + \log(g(a, t)!) \quad (3)$$

Here, $\sum_{a,t} \log(g(a, t)!)$ can be omitted since it does not affect the minimum. So, finally we arrive at

$$\mathcal{D}(f, \varphi) := \sum_{a,t} \hat{g}(a, t) - g(a, t) \log(\hat{g}(a, t)) \quad (4)$$

which is subject to minimization.

2.1.2 Regularization

Both image and motion suffer from the highly noisy data and have to be regularized. In case of the image, we apply moderate Gaussian smoothing (3 mm FWHM) after each image iteration.

In case of the motion function, we use homogeneous diffusion regularization in order to prevent extreme deformations [2] $\mathcal{S}(\varphi) = \sum_t \sum_{i=1}^3 \int \|\nabla_{\mathbf{x}}[\varphi]_i(\mathbf{x}, t)\|^2 d\mathbf{x}$; $\|\mathbf{a}\|$ is the euclidean norm of vector \mathbf{a} ($\|\mathbf{a}\| = \sqrt{\sum_i [\mathbf{a}]_i^2}$).

Finally, the complete cost functional we seek to minimize is

$$\mathcal{J}(f, \varphi) = \mathcal{D}(f, \varphi) + \alpha \mathcal{S}(\varphi) \quad (5)$$

The regularization parameter α defines the smoothness of our sought deformation. It has to be carefully adjusted to the specific case. If it is too high, the resulting φ will represent no visible deformation and thus the resulting image f will still suffer from motion blur. Is it too low, \mathcal{J} will be over-fitted and this will result in an unrealistic image and motion pair.

2.1.3 Optimization Scheme

The optimization scheme consists of alternating image and motion updates. An image update estimates the next image based on the current image and motion function. A motion update estimates the next motion function based on the current image and motion function. One JR iteration is defined as one image update followed by several motion updates. The motion updates are repeated until the maximal displacement is below 0.1 mm. In total we perform 60 JR iterations.

Since the image should not contain values below zero, we are confronted with a constrained optimization problem. Accordingly, the image update is derived by stating the Karush-Kuhn-Tucker conditions (necessary conditions for solutions for constrained optimization problems) and resolving them to an ML-EM like scheme. The motion update is a gradient descent scheme with adaptive stepsize. For details about the derivation, the reader is referred to [1].

2.2 Joint Reconstruction with Linear Diffusion Regularization (JR-LD)

As mentioned earlier, a disadvantage of putting the regularization directly in the objective functional is that we have to find the correct parameter α .

Therefore, we investigate an alternative approach. Instead of minimizing \mathcal{J} , we just minimize \mathcal{D} , without the smoothing term. After each motion update, we check whether the motion is invertible. If it is invertible, we just continue with the next JR iteration. If it is not invertible, we repeatedly smooth the motion with a small Gaussian kernel (with a FWHM of one pixel) until it is invertible. Note that repeated Gaussian smoothing is equivalent to Gaussian smoothing with a larger kernel. By choosing a small Gaussian kernel, we make sure that we do not smooth more than necessary in order to make the motion function invertible.

As an invertible criterion, we use the fact that the determinant of the Jacobian matrix (from now on just called the Jacobian) must be greater zero if and only if the motion is invertible. We calculate the Jacobian for every voxel position and check for this criterion.

2.3 Simulation

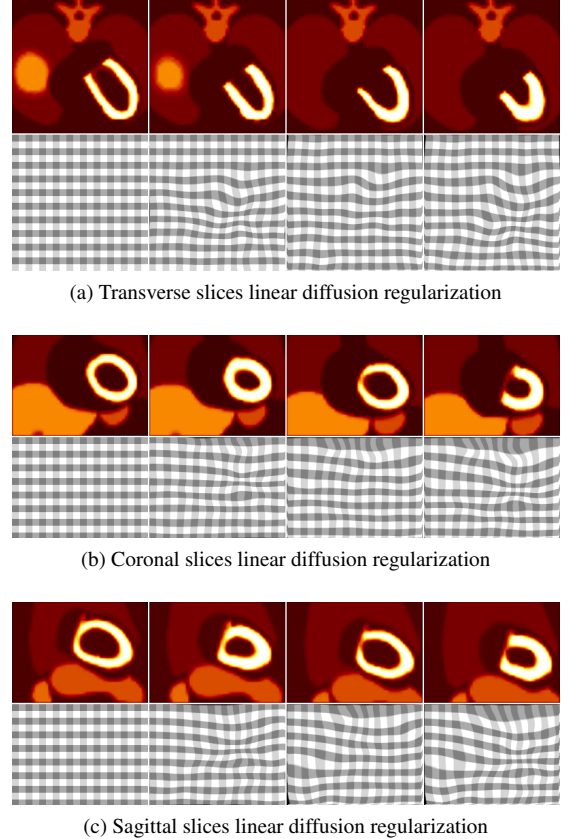


Figure 1: Generated original frames using the XCAT phantom.

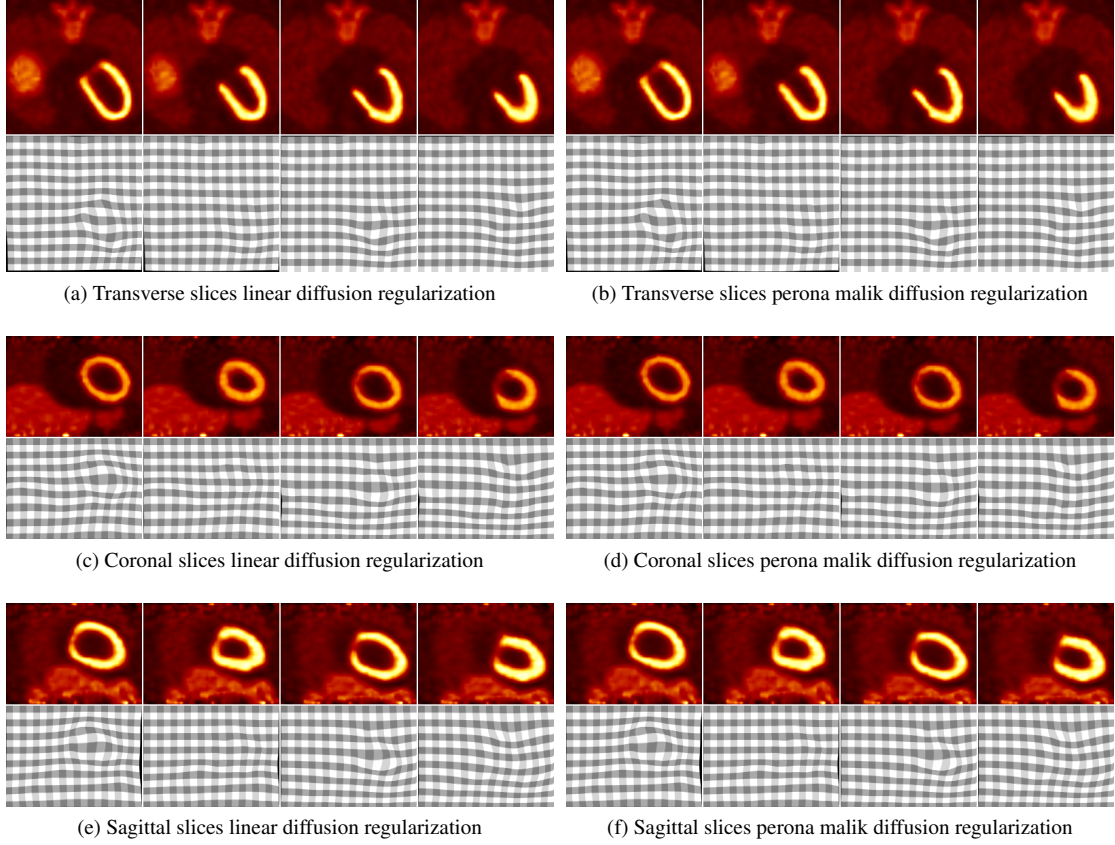


Figure 2: Reconstructed images by our joint reconstruction approach, with linear diffusion regularization and Perona-Malik diffusion regularization. There is no visual difference between the two reconstruction approaches.

We generate sixteen frames using the XCAT phantom [3]. For the sake of a better visualization, four of the sixteen frames are visualized in Figure 1. One complete respiratory cycle of a length of five seconds is simulated, together with five cardiac cycles of one second each. For the rest of the motion parameters, we use the standard parameters (e. g. the maximal diaphragm motion is 2 cm, the anteroposterior diameter of the ribcage, body, and lungs is 1.2 cm etc.). The activities of the organs are defined differently from the XCAT standard parameters: we use average ^{18}F standard uptake values measured for healthy patients [4].

The expected number of counts for each LOR is calculated by projecting each gate to measurement space using the system response function of the Siemens Biograph 16. The simulated measurements are finally generated from the expected number of counts by a Poisson random generator. In this way we take into account the acquisition time and activity. The number of simulated counts is 9×10^6 , which is a relatively low number and thus corresponds to a short acquisition time. Since we want to focus on image degradations induced by motion, we did not make use of Monte-Carlo simulation packages which could model effects like scattering, random coincidences, etc..

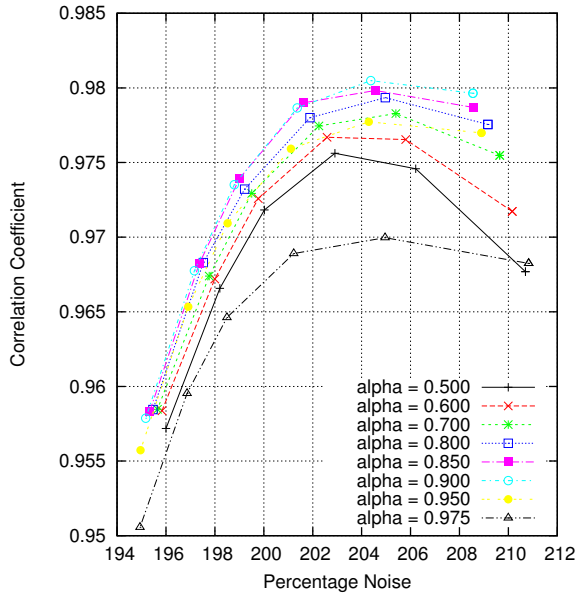
2.4 Evaluation

We compare the resulting images from JR-LD and JR-PMD to the original ground truth images by calculating the correlation coefficient. The correlation coefficient between two images \mathbf{x} and \mathbf{y} is defined as

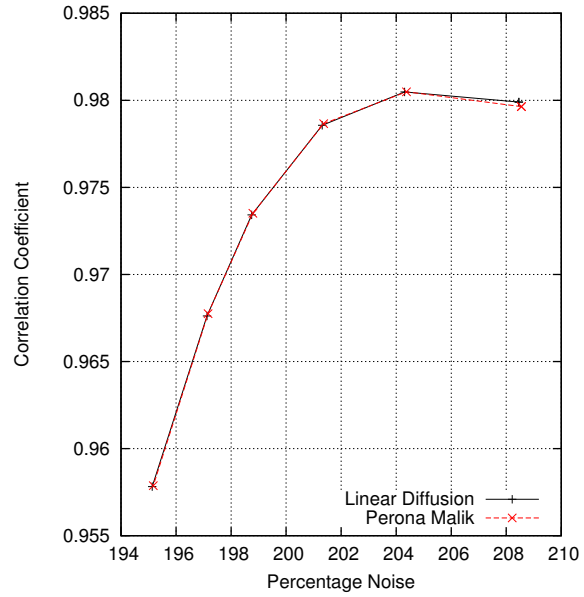
$$CC(\mathbf{x}, \mathbf{y}) = \frac{\mathbf{x}^\top \mathbf{y}}{\|\mathbf{x}\| \|\mathbf{y}\|} . \quad (6)$$

Both \mathbf{x} and \mathbf{y} are shifted such that their mean value is zero. The correlation coefficient ranges between -1 for totally anticorrelated images and 1 for perfectly correlated images.

Since the correlation coefficient depends heavily on the smoothness of the image, we have to make sure that we compare the images for the same level of background noise. We measure the noise by calculating the percent standard deviation (the standard deviation related to the mean value in percent) for a specific background region-of-interest (ROI). The reconstructed images are post-smoothed with differently sized Gaussian kernels, and the correlation coefficient calculated for each instance.



(a) JR-PMD reconstructions for different α



(b) JR-LD versus JR-PMD: almost equal

Figure 3: Background noise plotted versus correlation coefficient.

3 Results and Discussion

Figure 3a shows the different correlation curves for different values of the regularization parameter α used in the JR-PMD approach. This comparison is used in order to pick the best parameter $\alpha = 0.9$.

JR-PMD is compared to JR-LD in Figure 3b. Almost no quantitative difference is noted. This quantitative result is confirmed by 2, in which no difference between the two reconstruction approaches is visible.

4 Conclusions

We present a modified joint reconstruction algorithm which does not need a regularization parameter α . Since quantitative and visual evaluation shows that both the modified version and its original provide the same reconstruction quality, the modified version can be used instead. This is a big step towards practical use of joint reconstruction since the estimation of the correct parameter α is difficult, time consuming and error-prone.

References

- [1] M. Blume, A. Martinez-Möller, A. Keil, N. Navab, and M. Rafecas, "Joint reconstruction of image and motion in gated positron emission tomography," *to appear in IEEE Transactions on Medical Imaging*, 2010.
- [2] J. Modersitzki, *Numerical Methods for Image Registration*. Oxford University Press, 2004.
- [3] W. P. Segars, M. Mahesh, T. J. Beck, E. C. Frey, and B. M. W. Tsui, "Realistic CT simulation using the 4D XCAT phantom," *Medical Physics*, vol. 35, no. 8, pp. 3800–3808, 2008. [Online]. Available: <http://link.aip.org/link/?MPH/35/3800/1>
- [4] Y. Wang, E. Chiu, J. Rosenberg, and S. S. Gambhir, "Standardized uptake value atlas: Characterization of physiological 2-deoxy-2-[^{18}F]fluoro-d-glucose uptake in normal tissues," *Molecular Imaging and Biology*, vol. 9, no. 2, pp. 83–90, 3 2007.